Available online at www.sciencedirect.com
SCIENCE DIRECT®
ELSEVIER
International Journal of Solids and Structures 43 (2006) 4271–4296
INTERNATIONAL JOURNAL OF SOLIDS and STRUCTURES
www.elsevier.com/locate/ijsolstr

A new formulation for the analysis of elastic layers bonded to rigid surfaces

Seval Pinarbasi [a], Ugurhan Akyuz [a,*], Yalcin Mengi [b]

[a] *Department of Civil Engineering, Structural Mechanics Laboratory, Middle East Technical University, 06531 Ankara, Turkey*
[b] *Department of Engineering Sciences, Middle East Technical University, 06531 Ankara, Turkey*

Received 7 March 2005; received in revised form 17 June 2005
Available online 10 August 2005

Abstract

Elastic layers bonded to rigid surfaces have widely been used in many engineering applications. It is commonly accepted that while the bonded surfaces slightly influence the shear behavior of the layer, they can cause drastic changes on its compressive and bending behavior. Most of the earlier studies on this subject have been based on assumed displacement fields with assumed stress distributions, which usually lead to "average" solutions. These assumptions have somehow hindered the comprehensive study of stress/displacement distributions over the entire layer. In addition, the effects of geometric and material properties on the layer behavior could not be investigated thoroughly. In this study, a new formulation based on a modified Galerkin method developed by Mengi [Mengi, Y., 1980. A new approach for developing dynamic theories for structural elements. Part 1: Application to thermoelastic plates. International Journal of Solids and Structures 16, 1155–1168] is presented for the analysis of bonded elastic layers under their three basic deformation modes; namely, uniform compression, pure bending and apparent shear. For each mode, reduced governing equations are derived for a layer of arbitrary shape. The applications of the formulation are then exemplified by solving the governing equations for an infinite-strip-shaped layer. Closed form expressions are obtained for displacement/stress distributions and effective compression, bending and apparent shear moduli. The effects of shape factor and Poisson's ratio on the layer behavior are also investigated.

Keywords: Rubber; Bonded layer; Linear elasticity; Galerkin method; Compression; Bending; Apparent shear; Modulus; Infinite strip; Shape factor; Poisson's ratio

* Corresponding author. Tel.: +90 312 210 54 59; fax: +90 312 210 11 93.
E-mail address: han@metu.edu.tr (U. Akyuz).

0020-7683/$ - see front matter © 2005 Elsevier Ltd. All rights reserved.
doi:10.1016/j.ijsolstr.2005.06.047

1. Introduction

Elastic layers bonded to rigid surfaces (Fig. 1a) are widely used in many engineering applications, such as, for elastomeric bearings, sealing components or elastic foundations to machinery and motors. Earlier studies on this subject (e.g, Gent and Lindley, 1959; Chalhoub and Kelly, 1990) have clearly shown that rigid plates bonded to top and bottom faces of an elastic layer may cause considerable changes on the layer behavior. As an example, the compression or bending modulus of a bonded elastic layer may be several orders of magnitude greater than that of the corresponding unbonded layer due to the constraint of lateral expansion of material at the bonded surfaces. It is also known that the effects of bonded surfaces on layer behavior highly depend on the geometric and material properties of the layer, and becomes more pronounced when the material is nearly incompressible (Tsai and Lee, 1998; Koh and Lim, 2001).

As stated by Gent and Meinecke (1970), there are three basic deformation modes for a bonded elastic layer (Fig. 1a): uniform compression/extension, pure bending and apparent shear (Fig. 1b–d). Comprehensive analysis of a bonded elastic layer under its each deformation mode is essential for understanding the effects of bonded surfaces on its behavior, for studying the dependence of this behavior change on its geometric and material properties and for deriving closed form expressions for its stiffnesses; namely, *axial*, bending and *shear* stiffnesses, which are usually the key parameters in the design of mechanical and structural components composed of these units (Naeim and Kelly, 1999).

Many researchers have studied the compressive and/or bending behavior of bonded elastic layers, specifically bonded "rubber" layers. Most of these studies have been focused on the derivation of closed form expressions for their stiffnesses. Even though the behavior of rubber is indeed highly nonlinear and it may undergo considerable finite deformations, in most of the previous analytical treatments, rubber has been assumed to behave linearly and derivations have been made for small strains because the use of finite strain analysis with nonlinear constitutive models usually leads to highly nonlinear and complex equations (Kelly, 1997). In fact, in almost all cases, some additional simplifying assumptions have had to be made on the deformed shape and/or on the state of stress to obtain simple design formulas (Constantinou et al., 1992). It is also noteworthy that most of the initial studies on bonded rubber layers were based on the assumption of strict incompressibility, which has been shown by various experimental and analytical studies (e.g., Gent and Lindley, 1959; Koh and Kelly, 1989) to lead to the overestimation of true moduli, in particular, for "thin" layers.

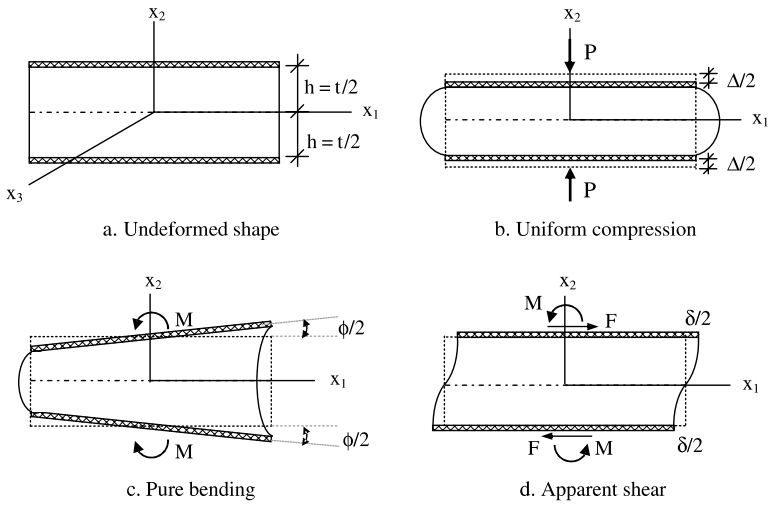

Fig. 1. Undeformed and deformed configurations of a bonded elastic layer under its three basic deformation modes.

Assuming strict incompressibility, Gent and Lindley (1959) derived approximate relations for the compression modulus of bonded infinitely long rectangular strips and circular discs. In their theoretical study, they considered that the total displacement of a bonded rubber layer is composed of the superposition of two simple displacements; pure homogeneous compression of the corresponding unbonded layer and additional displacement required to keep the points on the bonded surfaces in their original positions. This method of treatment, which has been later called the ''pressure method'', is based on three fundamental assumptions; (i) plane sections remain plane, (ii) lateral surfaces take a parabolic shape in the deformed configuration, (iii) normal stress components are all equal to the mean pressure. Gent and Lindley (1959) also recommended an ''ad-hoc'' modification to include the effect of bulk compressibility on compression modulus.

Gent and Meinecke (1970) extended the method of Gent and Lindley (1959) to the bonded elastic layers subject to bending and tabulated compression and bending stiffness factors for layers of various shape. Using an energy method and including compressibility effects, Lindley (1979a,b) derived closed form expressions for compression/bending modulus of infinite-strip-shaped bonded layers. Considering the material compressibility, Chalhoub and Kelly (1990) developed, by the pressure method, a theoretical approach to derive the compression/bending modulus of circular-shaped layers. This theoretical approach was later extended to the other geometric shapes (Chalhoub and Kelly, 1991; Constantinou et al., 1992; Kelly, 1997). Eliminating the stress assumption of the pressure method and using a direct solution formulated by means of either ''mean'' pressure or ''average'' horizontal displacements, Tsai and Lee (1998, 1999), Tsai (2003) and Tsai (2005) derived relations for the compression/bending modulus of bonded elastic layers of various shape. Using the same assumptions but through a variable transformation method, Koh and Kelly (1989) and Koh and Lim (2001) obtained solutions for the compression modulus of square and rectangular layers, respectively.

With a similar analytical approach for the derivation of radial and tilting stiffness of cylindrical rubber bush mountings, Horton et al. (2002a, 2003) derived closed form expressions for displacement/stress distributions and ''apparent Young's modulus'' for axially loaded rubber blocks in circular, annular and infinite-strip shapes. The main feature of the formulation of Horton et al. (2002a, 2003) is that while the assumption that plane sections remain plane is still kept in the formulation, the commonly used assumption of parabolic bulging shape is eliminated, which enabled the authors to investigate the validity of this assumption. The authors concluded that the shape of the bulging could not be approximated by a parabolic shape for considerably low shape factors (e.g., $S = 0.1$ or 0.2). Their results were in good agreement with the experimental results obtained by Mott and Roland (1995), who investigated the uniaxial behavior of very slender rubber cylinders (with $0.1 < S < 0.3$).

The studies conducted to investigate the compressive/bending behavior of bonded elastic layers are surely not limited only to the analytical studies. Several researchers (e.g., Holownia, 1972; Fenner and Remzi, 1983; Imbimbo and De Luca, 1998; Yeoh et al., 2002) studied the behavior of bonded elastic layers using numerical methods, such as, finite element, boundary element or dynamic relaxation methods. Main advantage of using these methods is that they do not usually include assumptions on neither displacement nor stress distributions. However, using numerical methods it is generally difficult and unpractical to study the behavior of bonded layers for various geometrical and material properties. Moreover, these solutions are also approximate and very sensitive to modelling.

In their common use, bonded elastic layers may also undergo shear deformations as shown in Fig. 1d. This deformation state is not ''simple shear'' due to the addition of bending deformations; it is named as ''apparent shear'' in literature. It is widely accepted that the effect of bonded surfaces to the shear behavior of the layer is negligible. This is a very realistic assumption for ''thin'' layers. However, as also stated by Gent and Meinecke (1970), bending displacements may become an important component of total displacement when the layer thickness is relatively large or when several thin layers are combined to form an assembly (e.g., elastomeric bearings). Although many analytical studies have been conducted on

compressive/bending behavior of bonded elastic layers, there is rather limited work in literature on their apparent shear behavior. Rivlin and Saunders (1949) studied experimentally the apparent shear behavior of cylindrical mountings with different geometries. They also suggested an approximate expression for the apparent shear modulus of bonded elastic layers using an approximate theory developed with the aid of the similarity of the problem to the problem of a cantilever beam loaded at its free end. Later, Gent and Meinecke (1970) recognized that Rivlin and Saunders (1949) ignored the effect of bonded surfaces to bending modulus and they proposed the use of modified bending modulus in Rivlin's formula. Recently, Horton et al. (2002b) studied the linear and incompressible behavior of circular-shaped rubber blocks under combined shear and bending. After obtaining general expressions, they examined three special loading cases: (a) pure bending, (b) cantilever loading and (c) apparent shear. Their expression for apparent shear modulus seems to have the same form with the expression proposed by Gent and Meinecke (1970). The basic difference in these expressions arises from the fact that while Gent and Meinecke's expression is derived based on parabolic bulging assumption, Horton et al. eliminated this assumption in their formulation.

In this study, a new analytical formulation is presented for the linear and small deformation analysis of bonded elastic layers under three basic deformation modes: uniform compression, pure bending and apparent shear. This new analytical treatment is formulated by using an approximate theory developed by Mengi (1980) using a modified version of the Galerkin method. As indicated by Papoulia and Kelly (1996), variational approaches, such as, the principle of minimum potential energy can also be used in the analysis of bonded layers. However, these approaches usually necessitate the selection of the form of displacement functions in advance to satisfy the displacement boundary conditions. Thus, their success generally depends on how well the behavior is guessed at the beginning. The approximate theory used in this study overcomes this difficulty; inclusion of the displacement boundary conditions in the formulation itself eliminates any possible inconsistency between the assumed displacement field and the boundary conditions at the bonded surfaces. How close to the exact solution is governed by the order of the theory. For this reason, for each deformation mode, the order of the theory is first left arbitrary and the relevant equations are presented in general forms, in view of displacement boundary conditions at the top and bottom faces of the layer. The constants which appear in the approximate theory are determined and tabulated by choosing the distribution functions employed in the theory as Legendre polynomials. Then, the application of the formulation is exemplified for each mode by solving the governing equations for a bonded layer of infinite-strip shape using zeroth and/or first order theories. Finally, for bonded strip layer, closed form expressions for displacement/stress distributions and for three effective moduli (compression, bending and apparent shear moduli) are presented, and the effects of shape factor (the ratio of one bonded area to bulge-to-free area) and Poisson's ratio on the layer behavior is studied.

2. Review of the approximate theory used in the study

In the present study, we employ an approximate theory proposed by Mengi (1980) for the dynamic behavior of the thermoelastic plates. The theory, developed by using a modified version of the Galerkin Method, assumes that the material is isotropic and linearly elastic and that the layer has a uniform thickness of $2h$. A Cartesian coordinate system (x_1 x_2 x_3) is defined at the mid-plane of the layer such that x_2 axis is perpendicular to the mid-plane (Fig. 1a). The approximate theory contains two types of field variables: ''generalized variables'' representing the weighted averages of displacements and stresses over the thickness of the layer, ''face variables'' representing the components of displacements and tractions on the lateral faces of the layer. The inclusion of face variables as field variables in theory eliminates any inconsistency which may exist between displacement distributions assumed over the thickness of the layer and boundary conditions on its flat faces. The theory due to Mengi (1980) differs in this respect from others available in literature.

In the development of the theory, a set of "distribution functions" $\{\phi_n(\bar{x}_2),\ n = 0, 1, 2, \ldots, \bar{x}_2 = x_2/h\}$ is chosen. The elements $\phi_n\,(n = 0, 1, \ldots, m+1, m+2)$ are retained in the set for mth order theory. Keeping the last two elements ϕ_{m+1} and ϕ_{m+2} in the set is essential for establishing the constitutive equations for face variables. The theory is composed of two sets of equations. The first set is derived by taking the weighted averages of elasticity equations with the use of $\phi_n\,(n = 0\text{–}m)$ as weighting functions. The second set of equations representing the "constitutive equations for face variables" is obtained through the expansion of displacements in terms of the distribution functions $\phi_n\,(n = 0\text{–}m+2)$ and using them in the exact constitutive equations of tractions on flat faces of the layer. With this procedure, the governing equations of the approximate theory are obtained in terms of some constants whose values can be computed once the distribution functions are selected.

In the present study, the approximate theory will be applied first in general terms to the formulation of some static deformation modes of a bonded elastic layer having arbitrary shape in horizontal plane; then, it will be used to obtain analytical expressions when the bonded layer is of strip shape (which involves 2D plane strain analysis). The extension of the analyses to other shapes (such as, square, rectangular, circular cylindrical layers) will be considered in a forthcoming paper (which involves 3D analysis). For this reason, to be used in both 2D and 3D analyses, in what follows the equations of the approximate theory are summarized for 3D case (for more details, see Mengi (1980)).

Written in indicial notation, the fundamental equations of linear elasticity, equilibrium (in the absence of body forces) and constitutive equations, are

$$\partial_j \tau_{ji} = 0 \quad (i, j = 1\text{–}3) \tag{1}$$

$$\tau_{ij} = \mu(\partial_i u_j + \partial_j u_i) + \delta_{ij}\lambda\partial_k u_k \quad (i, j = 1\text{–}3) \tag{2}$$

where λ and μ are Lamé's constants; u_i is displacement component; τ_{ij} is stress component; and δ_{ij} is the Kronecker delta. In writing Eqs. (1) and (2), the summation convention is used, where any repeated index indicates summation over its range. Moreover, ∂_i implies partial differentiation with respect to x_i.

The weighted averages of fundamental equations are established by applying the operator $L^n = \frac{1}{2h}\int_{-h}^{+h}(\cdot)\phi_n\,\mathrm{d}x_2$ with $n = 0\text{–}m$ to Eqs. (1) and (2), which gives

$$\partial_1 \tau_{1i}^n + \partial_3 \tau_{3i}^n + (R_i^n - \bar{\tau}_{2i}^n) = 0 \quad (n = 0\text{–}m) \tag{3}$$

where

$$R_i^n = \frac{\widehat{R}_i^n \phi_n(1)}{2h} \quad \text{where } \widehat{R}_i^n = \begin{cases} R_i^- = \tau_{2i}^+ - \tau_{2i}^- & \text{for even } n \\ R_i^+ = \tau_{2i}^+ + \tau_{2i}^- & \text{for odd } n \end{cases} \quad \text{with } \tau_{2i}^{\pm} = \tau_{2i}|_{x_2 = \pm h} \tag{4}$$

$$\bar{\tau}_{2i}^n = \overline{L}^n \tau_{2i} \quad \text{with } \overline{L}^n = \frac{1}{2h}\int_{-h}^{h}(\cdot)\frac{\mathrm{d}\phi_n}{\mathrm{d}x_2}\mathrm{d}x_2 \tag{5}$$

and

$$\begin{aligned}
\tau_{11}^n &= (2\mu + \lambda)\partial_1 u_1^n + \lambda\partial_3 u_3^n + \lambda(S_2^n - \bar{u}_2^n) \\
\tau_{22}^n &= \lambda(\partial_1 u_1^n + \partial_3 u_3^n) + (2\mu + \lambda)(S_2^n - \bar{u}_2^n) \\
\tau_{33}^n &= (2\mu + \lambda)\partial_3 u_3^n + \lambda\partial_1 u_1^n + \lambda(S_2^n - \bar{u}_2^n) \\
\tau_{12}^n &= \mu\partial_1 u_2^n + \mu(S_1^n - \bar{u}_1^n) \\
\tau_{13}^n &= \mu\partial_1 u_3^n + \mu\partial_3 u_1^n \\
\tau_{23}^n &= \mu\partial_3 u_2^n + \mu(S_3^n - \bar{u}_3^n) \quad (n = 0\text{–}m)
\end{aligned} \tag{6}$$

where

$$S_i^n = \frac{\widehat{S}_i^n \phi_n(1)}{2h} \quad \text{where } \widehat{S}_i^n = \begin{cases} S_i^- = u_i^+ - u_i^- & \text{for even } n \\ S_i^+ = u_i^+ + u_i^- & \text{for odd } n \end{cases} \quad \text{with } u_i^\pm = u_i|_{x_2=\pm h}$$
$$\bar{u}_i^n = \overline{L}^n u_i \tag{7}$$

In the derivation of Eqs. (3)–(7), it is assumed that ϕ_n is even function of $\bar{x}_2$ for even n and odd function of $\bar{x}_2$ for odd n. Also, it may be assumed without loss of generality that $\phi_n' = \frac{d\phi_n}{d\bar{x}_2}$ is related to ϕ_j by $\phi_n' = \sum_{j=0}^m c_{nj}\phi_j$, implying that $\bar{\tau}_{2i}^n$ and $\bar{u}_i^n$ are related to τ_{2i}^n and u_i^n by Eq. (8) in which the constants c_{nj} may be computed whenever the distribution functions are selected.

$$(\bar{\tau}_{2i}^n, \bar{u}_i^n) = \frac{1}{h}\sum_{j=0}^m c_{nj}(\tau_{2i}^j, u_i^j) \tag{8}$$

For the derivation of the constitutive equations for face variables $R_i^\pm$, displacements u_i are expanded in terms of ϕ_k ($k = 0, 1, 2, \ldots, m+2$) as

$$u_i = \sum_{k=0}^{m+2} a_k^i \phi_k \tag{9}$$

where a_k^i are some coefficients which are functions of x_1 and x_3. It is to be noted that Eq. (9) is not an assumption for the shape of displacements u_i over the thickness of the layer; it is the representation of u_i in terms of complete shape (base) functions ϕ_i, in fact, this representation would be exact for $m \to \infty$. When L^n ($n = 0$–m) operator is applied to this expression, one obtains

$$u_i^n = \sum_{k=0}^{m+2} d_{nk} a_k^i \quad \text{where } d_{nk} = L^n\phi_k = \frac{1}{2h}\int_{-h}^{h} \phi_n \phi_k \, dx_2 \tag{10}$$

Assumed properties of ϕ_k lead to the following uncoupled system of equations for the determination of coefficients a_k^i:

$$\begin{aligned} &u_i^n = \sum_{k=0,2}^{p+2} d_{nk} a_k^i \quad \text{and} \quad \frac{S_i^+}{2} = \sum_{k=0,2}^{p+2} a_k^i \phi_k(1) \quad (n = 0, 2, \ldots, p) \quad \text{for even } k \\ &u_i^n = \sum_{k=1,3}^{p'+2} d_{nk} a_k^i \quad \text{and} \quad \frac{S_i^-}{2} = \sum_{k=1,3}^{p'+2} a_k^i \phi_k(1) \quad (n = 1, 3, \ldots, p') \quad \text{for odd } k \end{aligned} \tag{11}$$

where $p = m$ and $p' = m - 1$ for even m and $p = m - 1$ and $p' = m$ for odd m. From the solutions of above equations, the coefficients a_k^i are determined in terms of u_i^n and $S_i^\pm$ as

$$a_k^i = \sum_{j=0,2}^{p} f_{kj} u_i^j + f_{k,p+2} S_i^+ \quad \text{for even } k \quad \text{and} \quad a_k^i = \sum_{j=1,3}^{p'} f_{kj} u_i^j + f_{k,p'+2} S_i^- \quad \text{for odd } k \tag{12}$$

where the coefficients f_{kj} ($k,j = 0$–$m+2$) may be computed whenever ϕ_n are chosen.

Finally, to obtain the constitutive equations for face variables, one should use Eq. (9) in $R_i^\pm = \tau_{2i}^+ \pm \tau_{2i}^-$ with $\tau_{2i} = \mu(\partial_2 u_i + \partial_i u_2) + \lambda\delta_{i2}\partial_k u_k$, which gives

$$
\begin{aligned}
R_1^+ &= \mu(\partial_1 S_2^+) + \frac{2\mu}{h}\left(\sum_{k=1,3}^{p'} \gamma_k u_1^k + \gamma^- S_1^-\right)\\
R_1^- &= \mu(\partial_1 S_2^-) + \frac{2\mu}{h}\left(\sum_{k=0,2}^{p} \gamma_k u_1^k + \gamma^+ S_1^+\right)\\
R_2^+ &= \lambda(\partial_1 S_1^+ + \partial_3 S_3^+) + \frac{2(2\mu+\lambda)}{h}\left(\sum_{k=1,3}^{p'} \gamma_k u_2^k + \gamma^- S_2^-\right)\\
R_2^- &= \lambda(\partial_1 S_1^- + \partial_3 S_3^-) + \frac{2(2\mu+\lambda)}{h}\left(\sum_{k=0,2}^{p} \gamma_k u_2^k + \gamma^+ S_2^+\right)\\
R_3^+ &= \mu(\partial_3 S_2^+) + \frac{2\mu}{h}\left(\sum_{k=1,3}^{p'} \gamma_k u_3^k + \gamma^- S_3^-\right)\\
R_3^- &= \mu(\partial_3 S_2^-) + \frac{2\mu}{h}\left(\sum_{k=0,2}^{p} \gamma_k u_3^k + \gamma^+ S_3^+\right)
\end{aligned}
\tag{13}
$$

where

$$
\begin{aligned}
&\gamma_j = \sum_{k=1,3}^{p'+2} f_{kj}\phi_k'(1) \quad \text{for } j = 1,3,\ldots,p' \quad \text{and} \quad \gamma_j = \sum_{k=0,2}^{p+2} f_{kj}\phi_k'(1) \quad \text{for} \quad j = 0,2,\ldots,p\\
&\gamma^- = \sum_{k=1,3}^{p'+2} f_{k,p'+2}\phi_k'(1), \quad \gamma^+ = \sum_{k=0,2}^{p+2} f_{k,p+2}\phi_k'(1)
\end{aligned}
\tag{14}
$$

In the approximate theory, the weighted forms of the equilibrium equations [$3(m+1)$ equations] and constitutive equations [$6(m+1)$ equations] provide [$9(m+1)$] equations. In addition, six equations come from the boundary conditions at the top and bottom faces of the layer. These boundary conditions specify one of the traction or displacement components, or their combination, in each direction on each face of the layer. On the other hand, the constitutive equations for face variables provide six more equations. Thus, the number of available equations in the approximate theory is [$9(m+1)+12$], which is sufficient to compute the unknowns $(\tau_{ij}^n, u_i^n, S_i^{\pm}, R_i^{\pm})$, whose number is also [$9(m+1)+12$].

3. Application of the approximate theory to bonded elastic layers

Fig. 1a shows the undeformed configuration of an elastic layer of uniform thickness t bonded to rigid plates at its top and bottom faces. The deformed configurations of the layer under three fundamental deformation modes are shown in Fig. 1b–d. In the first deformation mode (Fig. 1b), the layer is compressed uniformly by a uniaxial compressive force P such that the bonded faces approach uniformly towards each other with a relative vertical displacement Δ. In the second deformation mode (Fig. 1c), the layer is purely bended by bending moments M so that the bonded faces rotate with respect to each other about x_3 axis with a relative angle of rotation ϕ. Finally, in the third mode (Fig. 1d), the bonded layer is subjected to the combined effects of shearing force F and bending moments $M = tF/2$ so that the bonded faces move with respect to each other in horizontal direction with a relative horizontal displacement δ. The object is to formulate and analyze each problem within the framework of the approximate theory presented in the previous section. In the analyses, the layer will be referred to the same rectangular frame employed in the approximate theory. In the derivations and results presented in subsequent sections, the distribution

Table 1
c_{nj} coefficients (ϕ_n's are Legendre polynomials)

n	j				
	0	1	2	3	4
0	0	0	0	0	0
1	1	0	0	0	0
2	0	3	0	0	0
3	1	0	5	0	0
4	0	3	0	7	0

Table 2
Coefficients a_k^i and constants γ_j, $\gamma^{\pm}$ for the 0th, 1st and 2nd order theories (ϕ_n's are Legendre polynomials)

m	a_k^i $(k = 0{-}m+2)$	$\gamma_j (j = 0{-}m)$	γ^+	γ^-
0	$\begin{bmatrix} u_i^0 \\ S_i^-/2 \\ S_i^+/2 - u_i^0 \end{bmatrix}$	$\{-3\}$	3/2	1/2
1	$\begin{bmatrix} u_i^0 \\ 3u_i^1 \\ S_i^+/2 - u_i^0 \\ S_i^-/2 - 3u_i^1 \end{bmatrix}$	$\begin{Bmatrix} -3 \\ -15 \end{Bmatrix}$	3/2	3
2	$\begin{bmatrix} u_i^0 \\ 3u_i^1 \\ 5u_i^2 \\ S_i^-/2 - 3u_i^1 \\ S_i^+/2 - 5u_i^2 - u_i^0 \end{bmatrix}$	$\begin{Bmatrix} -10 \\ -15 \\ -35 \end{Bmatrix}$	5	3

functions in the approximate theory are chosen as Legendre polynomials of the first kind. The coefficients c_{nj}, a_k^i, γ_j and $\gamma^{\pm}$ of the theory for these distribution functions are listed in Tables 1 and 2. It is worth to be noted that any distribution functions ϕ_n may be chosen in the approximate theory as long as they form a complete set implying that the prediction of the approximate theory approaches the actual response as the number of terms in the set $\{\phi_n\}$ increases. Legendre polynomials, $P_n(x_2)$, selected as distribution functions in the present study, are orthogonal implying that the completeness of the set $\{\phi_n\}$ is satisfied automatically with this choice of $\{\phi_n\}$; besides, the orthogonality of P_n facilitates the computations of constants appearing in the approximate theory.

3.1. Derivation of reduced governing equations

3.1.1. Uniform compression

From the deformed configuration of a concentrically compressed elastic layer shown in Fig. 1b, it is clear that the vertical displacement component u_2 is antisymmetric whereas the horizontal displacement components u_1 and u_3 are symmetric about the mid-plane of the layer. Since the distribution functions, are even functions of $\bar{x}_2$ for even n, and odd functions of $\bar{x}_2$ for odd n, one has

$$\begin{aligned} u_1^n = u_3^n = 0 \quad \text{and} \quad \bar{u}_2^n = 0 \quad \text{for odd } n \\ \bar{u}_1^n = \bar{u}_3^n = 0 \quad \text{and} \quad u_2^n = 0 \quad \text{for even } n \end{aligned} \tag{15}$$

Furthermore, since the elastic layer is bonded at its top and bottom face, the material points at the bonded faces can only displace uniformly in the axial direction; this implies that

$$u_1^{\pm} = u_3^{\pm} = 0 \quad \text{and} \quad u_2^{\pm} = u_2|_{x_2=\pm h} = \mp\frac{\Delta}{2} \tag{16}$$

which leads to

$$S_1^{\pm} = S_3^{\pm} = S_2^{+} = 0 \quad \text{and} \quad S_2^{-} = -\Delta \tag{17}$$

from which it is obvious that

$$\begin{aligned} &S_1^n = S_3^n = 0 \quad \text{for all} \quad n, \quad S_2^n = \begin{cases} -\Delta/t & \text{for even } n \\ 0 & \text{for odd } n \end{cases} \\ &(\partial_1 S_i^n, \partial_3 S_i^n) = 0 \quad \text{for } i = 1\text{–}3 \quad \text{for all } n \end{aligned} \tag{18}$$

Then, the constitutive equations for face variables and the weighted form of constitutive equations have the following uncoupled forms:

- *constitutive equations for face variables:*

$$R_i^n = \frac{4\mu}{t^2}\left(\sum_{k=0,2}^{p} \gamma_k u_i^k\right) \quad (i = 1, 3) \quad \text{for even } n, \qquad R_2^n = \frac{4\alpha}{t^2}\left(\sum_{k=1,3}^{p'} \gamma_k u_2^k - \Delta\gamma^-\right) \quad \text{for odd } n \tag{19}$$

- *weighted constitutive equations:*

$$\left.\begin{aligned} \tau_{11}^n &= \alpha\partial_1 u_1^n + \lambda\partial_3 u_3^n - \frac{\lambda\Delta}{t} - \lambda\bar{u}_2^n \\ \tau_{22}^n &= \lambda\partial_1 u_1^n + \lambda\partial_3 u_3^n - \frac{\alpha\Delta}{t} - \alpha\bar{u}_2^n \\ \tau_{33}^n &= \lambda\partial_1 u_1^n + \alpha\partial_3 u_3^n - \frac{\lambda\Delta}{t} - \lambda\bar{u}_2^n \\ \tau_{13}^n &= \mu\partial_1 u_3^n + \mu\partial_3 u_1^n \end{aligned}\right\} \quad \text{for even } n$$

$$\left.\begin{aligned} \tau_{12}^n &= \mu\partial_1 u_2^n - \mu\bar{u}_1^n \\ \tau_{23}^n &= \mu\partial_3 u_2^n - \mu\bar{u}_3^n \end{aligned}\right\} \quad \text{for odd } n \tag{20}$$

where $\alpha = 2\mu + \lambda$, and other R_i^n and τ_{ij}^n being zero.

Substitution of Eqs. (19) and (20) into Eq. (3) gives the following governing equations for weighted displacements u_i^n:

$$\left.\begin{aligned} &\alpha\partial_{11}u_1^n + \mu\partial_{33}u_1^n + (\lambda+\mu)\partial_{13}u_3^n - \lambda\partial_1\bar{u}_2^n + \frac{4\mu}{t^2}\left(\sum_{k=0,2}^{p}\gamma_k u_1^k\right) = \bar{\tau}_{21}^n \\ &\alpha\partial_{33}u_3^n + \mu\partial_{11}u_3^n + (\lambda+\mu)\partial_{13}u_1^n - \lambda\partial_3\bar{u}_2^n + \frac{4\mu}{t^2}\left(\sum_{k=0,2}^{p}\gamma_k u_3^k\right) = \bar{\tau}_{23}^n \end{aligned}\right\} \quad \text{for even } n$$

$$\mu\partial_{11}u_2^n + \mu\partial_{33}u_2^n - \mu\partial_1\bar{u}_1^n - \mu\partial_3\bar{u}_3^n + \frac{4\alpha}{t^2}\left(\sum_{k=1,3}^{p'}\gamma_k u_2^k\right) - \frac{4\alpha}{t^2}\Delta\gamma^- = \bar{\tau}_{22}^n \quad \text{for odd } n \tag{21}$$

where $\bar{u}_i^n$ and $\bar{\tau}_{2i}^n$ are related to u_i^n and τ_{2i}^n by, in view of Eq. (8),

$$(\bar{u}_i^n, \bar{\tau}_{2i}^n) = \frac{2}{t}\sum_{j=0}^{m} c_{nj}(u_i^j, \tau_{2i}^j) \tag{22}$$

in which τ_{2i}^{j} can be expressed in terms of u_i^n by Eqs. (20). Eqs. (21) with Eqs. (20) and (22) comprise the reduced governing equations for the problem of uniform compression of bonded elastic layers.

3.1.2. Pure bending

Similar to the uniform compression case, under pure bending, the vertical displacement u_2 is antisymmetric while the horizontal displacements u_1 and u_3 are symmetric about the mid-plane of the layer (Fig. 1c). Therefore, Eqs. (15) are valid also for the bending problem, for which the displacement boundary conditions at the bonded faces of the layer are

$$u_1^{\pm} = u_3^{\pm} = 0 \quad \text{and} \quad u_2^{\pm} = u_2|_{x_2=\pm h} = \pm\frac{\phi}{2}x_1 \tag{23}$$

which leads to

$$S_1^{\pm} = S_3^{\pm} = S_2^{+} = 0 \quad \text{and} \quad S_2^{-} = \phi x_1 \tag{24}$$

Then,

$$S_1^n = S_3^n = 0 \quad \text{for all } n, \quad S_2^n = \begin{cases} \phi x_1/t & \text{for even } n \\ 0 & \text{for odd } n \end{cases} \tag{25}$$

Substituting Eqs. (15), (24) and (25) into the governing equations of the theory and following the same procedure described in Section 3.1.1, one can obtain the reduced form of the governing equations for this bending problem as

- *weighted equilibrium equations:*

$$\left.\begin{aligned} &\alpha\partial_{11}u_1^n + \mu\partial_{33}u_1^n + (\lambda+\mu)\partial_{13}u_3^n - \lambda\partial_1\bar{u}_2^n + \frac{4\mu}{t^2}\left(\sum_{k=0,2}^{p}\gamma_k u_1^k\right) + (\lambda+\mu)\frac{\phi}{t} = \bar{\tau}_{21}^n \\ &\alpha\partial_{33}u_3^n + \mu\partial_{11}u_3^n + (\lambda+\mu)\partial_{13}u_1^n - \lambda\partial_3\bar{u}_2^n + \frac{4\mu}{t^2}\left(\sum_{k=0,2}^{p}\gamma_k u_3^k\right) + \mu\frac{\phi}{t} = \bar{\tau}_{23}^n \end{aligned}\right\} \quad \text{for even } n$$

$$\mu\partial_{11}u_2^n + \mu\partial_{33}u_2^n - \mu\partial_1\bar{u}_1^n - \mu\partial_3\bar{u}_3^n + \frac{4\alpha}{t^2}\left(\sum_{k=1,3}^{p'}\gamma_k u_2^k\right) + \frac{4\alpha}{t^2}\gamma^{-}\phi x_1 = \bar{\tau}_{22}^n \quad \text{for odd } n \tag{26}$$

- *weighted constitutive equations:*

$$\left.\begin{aligned} \tau_{11}^n &= \alpha\partial_1 u_1^n + \lambda\partial_3 u_3^n + \frac{\lambda\phi}{t}x_1 - \lambda\bar{u}_2^n \\ \tau_{22}^n &= \lambda\partial_1 u_1^n + \lambda\partial_3 u_3^n + \frac{\alpha\phi}{t}x_1 - \alpha\bar{u}_2^n \\ \tau_{33}^n &= \lambda\partial_1 u_1^n + \alpha\partial_3 u_3^n + \frac{\lambda\phi}{t}x_1 - \lambda\bar{u}_2^n \\ \tau_{13}^n &= \mu\partial_1 u_3^n + \mu\partial_3 u_1^n \end{aligned}\right\} \quad \text{for even } n$$

$$\left.\begin{aligned} \tau_{12}^n &= \mu\partial_1 u_2^n - \mu\bar{u}_1^n \\ \tau_{23}^n &= \mu\partial_3 u_2^n - \mu\bar{u}_3^n \end{aligned}\right\} \quad \text{for odd } n \tag{27}$$

In Eqs. (26), $\bar{u}_i^n$ and $\bar{\tau}_{2i}^n$ are related to u_i^n and τ_{2i}^n by Eq. (22) and τ_{2i}^j can be expressed in terms of u_i^n by Eqs. (27).

3.1.3. Apparent shear

Apparent shear of the layer shown in Fig. 1a results in the deformed shape shown in Fig. 1d, from which it is obvious that the boundary conditions at the bonded faces are

$$u_1^{\pm} = u_1|_{x_2=\pm h} = \pm\frac{\delta}{2} \quad \text{and} \quad u_2^{\pm} = u_3^{\pm} = 0 \tag{28}$$

Then,

$$\begin{aligned} &S_1^{+} = S_2^{\pm} = S_3^{\pm} = 0 \quad \text{and} \quad S_1^{-} = \delta \\ &S_2^n = S_3^n = 0 \quad \text{for all } n, \quad S_1^n = \begin{cases} \delta/t & \text{for even } n \\ 0 & \text{for odd } n \end{cases} \end{aligned} \tag{29}$$

Contrary to the compression and bending cases, under apparent shear, the vertical displacement u_2 is symmetric whereas the horizontal displacements u_1 and u_3 are antisymmetric about the mid-plane of the layer. That is,

$$\begin{aligned} &u_1^n = u_3^n = 0 \quad \text{and} \quad \bar{u}_2^n = 0 \quad \text{for even } n \\ &\bar{u}_1^n = \bar{u}_3^n = 0 \quad \text{and} \quad u_2^n = 0 \quad \text{for odd } n \end{aligned} \tag{30}$$

Following the same procedure employed in Section 3.1.1, the governing equations for the apparent shear problem may be obtained as

- *weighted form of equilibrium equations:*

$$\left.\begin{aligned} &\alpha\partial_{11}u_1^n + \mu\partial_{33}u_1^n + (\lambda+\mu)\partial_{13}u_3^n - \lambda\partial_1\bar{u}_2^n + \frac{4\mu}{t^2}\left(\sum_{k=1,3}^{p'}\gamma_k u_1^k\right) + \frac{4\mu}{t^2}\delta\gamma^{-} = \bar{\tau}_{21}^n \\ &\alpha\partial_{33}u_3^n + \mu\partial_{11}u_3^n + (\lambda+\mu)\partial_{13}u_1^n - \lambda\partial_3\bar{u}_2^n + \frac{4\mu}{t^2}\left(\sum_{k=1,3}^{p'}\gamma_k u_3^k\right) = \bar{\tau}_{23}^n \end{aligned}\right\} \quad \text{for odd } n$$

$$\mu\partial_{11}u_2^n + \mu\partial_{33}u_2^n - \mu\partial_1\bar{u}_1^n - \mu\partial_3\bar{u}_3^n + \frac{4\alpha}{t^2}\left(\sum_{k=0,2}^{p}\gamma_k u_2^k\right) = \bar{\tau}_{22}^n \quad \text{for even } n \tag{31}$$

- *weighted form of constitutive equations:*

$$\left.\begin{aligned} \tau_{11}^n &= \alpha\partial_1 u_1^n + \lambda\partial_3 u_3^n - \lambda\bar{u}_2^n \\ \tau_{22}^n &= \lambda\partial_1 u_1^n + \lambda\partial_3 u_3^n - \alpha\bar{u}_2^n \\ \tau_{33}^n &= \lambda\partial_1 u_1^n + \alpha\partial_3 u_3^n - \lambda\bar{u}_2^n \\ \tau_{13}^n &= \mu\partial_1 u_3^n + \mu\partial_3 u_1^n \end{aligned}\right\} \quad \text{for even } n$$

$$\left.\begin{aligned} \tau_{12}^n &= \mu\partial_1 u_2^n - \mu\bar{u}_1^n + \mu\tfrac{\delta}{t} \\ \tau_{23}^n &= \mu\partial_3 u_2^n - \mu\bar{u}_3^n \end{aligned}\right\} \quad \text{for odd } n \tag{32}$$

In Eq. (31), $\bar{u}_i^n$ and $\bar{\tau}_{2i}^n$ are related to u_i^n and τ_{2i}^n by Eq. (22) and τ_{2i}^j can be expressed in terms of u_i^n by Eqs. (32).

3.2. Determination of displacement/stress distributions

Eqs. (21), (26) and (31) constitute three sets of partial differential equations for weighted displacements u_i^n, governing the behavior of a bonded elastic layer under its three basic deformation modes. Necessary boundary conditions for the solution of these differential equations are the traction-free boundary conditions at the lateral bulge-free surfaces. Once the governing equations are solved for u_i^n subject to these boundary conditions, determination of displacements, stress distributions or any other parameter, such as, stiffness of the bonded layer is straightforward.

For various orders of the theory, the distributions of displacements $u_i (i = 1\text{–}3)$ may be computed in terms of u_i^n and $S_i^{\pm}$ as, in view of the coefficients in Table 2 and of Eq. (9),

$$
\begin{aligned}
u_i &= u_i^0 + \left(\frac{S_i^-}{2}\right)\left(\frac{2x_2}{t}\right) + \left(\frac{S_i^+}{2} - u_i^0\right)\left(\frac{6x_2^2}{t^2} - \frac{1}{2}\right) \quad \text{for } m = 0 \\
u_i &= u_i^0 + (3u_i^1)\left(\frac{2x_2}{t}\right) + \left(\frac{S_i^+}{2} - u_i^0\right)\left(\frac{6x_2^2}{t^2} - \frac{1}{2}\right) + \left(\frac{S_i^-}{2} - 3u_i^1\right)\left(\frac{20x_2^3}{t^3} - \frac{3x_2}{t}\right) \quad \text{for } m = 1 \\
u_i &= \left\{ \begin{array}{l} u_i^0 + (3u_i^1)\left(\frac{2x_2}{t}\right) + (5u_i^2)\left(\frac{6x_2^2}{t^2} - \frac{1}{2}\right) + \left(\frac{S_i^-}{2} - 3u_i^1\right)\left(\frac{20x_2^3}{t^3} - \frac{3x_2}{t}\right) \\ \quad + \left(\frac{S_i^+}{2} - u_i^0 - 5u_i^2\right)\left(\frac{70x_2^4}{t^4} - \frac{15x_2^2}{t^2} + \frac{3}{8}\right) \end{array} \right\} \quad \text{for } m = 2
\end{aligned}
\tag{33}
$$

Substitution of these displacements into Eq. (2) determines the stress distributions.

3.3. Compression, bending and apparent shear moduli

The effective modulus of the layer under its any deformation state may be determined whenever the stress distributions are determined. Effective compression modulus E_c of a bonded elastic layer can be obtained from the ratio of nominal compressive stress, defined as the ratio of applied axial load P to the undeformed horizontal sectional area A of the layer, to nominal compressive strain, defined as the ratio of total compression of the layer, Δ, to its initial thickness. Thus, for the effective compression modulus E_c, one has

$$
E_c = \frac{P}{A\varepsilon_c} \quad \text{where } \varepsilon_c = \frac{\Delta}{t} \tag{34}
$$

Similarly, the effective bending modulus of the layer E_b can be determined from the ratio of bending stiffness K_b, defined as the ratio of the applied moment M to the resultant curvature κ, to the moment of inertia I of the layer about the axis of rotation. Thus, the effective bending modulus E_b is given by

$$
E_b = \frac{K_b}{I} \quad \text{where } K_b = \frac{M}{\kappa} \quad \text{with } \kappa = \frac{\phi}{t} \tag{35}
$$

Determination of apparent shear modulus μ_a of the layer is very similar to that of compression modulus. It is simply the ratio of nominal shear stress τ to nominal shear strain γ, that is,

$$
\mu_a = \frac{\tau}{\gamma} \quad \text{where } \tau = \frac{F}{A} \quad \text{and} \quad \gamma = \frac{\delta}{t} \tag{36}
$$

For any deformation state, applied load can be computed by integrating the related face stress $\tau_{2i}^{\pm}$ over the horizontal section of the layer. Similarly, applied moment can be determined by integrating, over horizontal area, the moment of the related face stress about centroidal axis. Since the zeroth order theory corresponds to the averaging of the variables through the layer thickness, τ_{2i}^0, instead of $\tau_{2i}^{\pm}$, should be used in the calculation of forces/moments for this order. Thus, the compressive force P, bending moment M and shear force F in Eqs. (34)–(36) may be obtained from

$$
\begin{aligned}
(P, M, F) &= \int\int_A (-\tau_{22}^0, \tau_{22}^0 x_1, \tau_{12}^0)\, \mathrm{d}A \quad \text{for } m = 0 \\
(P, M, F) &= \int\int_A (-\tau_{22}^{\pm}, \tau_{22}^{\pm} x_1, \tau_{12}^{\pm})\, \mathrm{d}A \quad \text{for } m = 1, 2, \ldots
\end{aligned}
\tag{37}
$$

where, in view of that $R_2^- = \tau_{22}^+ - \tau_{22}^- = 0$ for uniform compression and pure bending problems, and $R_1^- = \tau_{12}^+ - \tau_{12}^- = 0$ and $R_2^+ = \tau_{22}^+ + \tau_{22}^- = 0$ for apparent shear problem,

$$\left.\begin{aligned} \tau_{22}^{\pm} &= \frac{2\alpha}{t}\left(\sum_{k=1,3}^{p'}\gamma_k u_2^k\right) + \frac{2\alpha}{t}\gamma^- \beta \quad \text{where } \beta = \begin{cases} -\Delta & \text{for uniform compression} \\ \phi x_1 & \text{for pure bending} \end{cases} \\ \tau_{22}^{+} &= -\tau_{22}^{-} = \frac{2\alpha}{t}\left(\sum_{k=0,2}^{p}\gamma_k u_2^k\right) \\ \tau_{12}^{\pm} &= \frac{2\mu}{t}\left(\sum_{k=1,3}^{p'}\gamma_k u_1^k\right) + \frac{2\mu}{t}\gamma^- \delta \end{aligned}\right\} \quad \text{for apparent shear} \tag{38}$$

4. Application of the formulation to the infinite-strip-shaped bonded elastic layers

Above three sets of governing equations corresponding to three fundamental deformation states are derived for a bonded elastic layer of any arbitrary shape. The formulation can easily be applied to a layer of any shape to analyze its behavior under its basic deformation modes. The solutions obtained for each mode can surely be superposed to analyze the effect of bonded surfaces on more complex behavior of the layer under combined loadings.

In this study, the formulation presented in the previous section is applied to infinite-strip-shaped bonded layers. For each deformation mode, governing equations are solved for displacements, from which closed form expressions for stress distributions and relevant modulus are derived.

In the analysis presented in the following sections, it is assumed that the length of the bonded rectangular layer is much larger than its width $2w$ and thickness t. It is clear that this layer may be approximated by an infinite-strip-shaped bonded layer in a state of plane strain. When the centerline of the strip is taken to coincide with x_3 axis, one has $u_3 = 0$. Moreover, the nonzero displacements are independent of x_3; i.e., $u_1 = u_1(x_1, x_2), u_2 = u_2(x_1, x_2)$. Only the compression problem is solved by using both zeroth and first order theories. After showing that zeroth order theory indeed results in the same solutions obtained in literature by the formulations which "average" the variables through the layer thickness, the bending and apparent shear problems are solved by using only the first order theory.

4.1. Solutions of governing equations

4.1.1. Uniform compression

4.1.1.1. Solution for zeroth order theory. For the zeroth order theory ($m = 0$, $p = 0$ and $p' = -1$), the weighted equilibrium equation in x_2 direction (third of Eqs. (21)) is trivially satisfied. In view of Eq. (22) and Tables 1, 2 for $m = 0$, the weighted form of the equilibrium equation in x_1 direction (first of Eq. (21)) becomes

$$\partial_{11} u_1^0 - \beta_{10}^2 u_1^0 = 0 \quad \text{with } \beta_{10}^2 = \frac{12\mu}{\alpha t^2} \tag{39}$$

Since u_1 is antisymmetric about $x_1 = 0$, the solution of Eq. (39) for u_1^0 is

$$u_1^0 = a_{10}\sinh(\beta_{10} x_1) \tag{40}$$

where a_{10} is an integration constant which can be determined from the traction-free boundary conditions $\tau_{12}^0|_{x_1=\pm w} = 0$ and $\tau_{11}^0|_{x_1=\pm w} = 0$ at the lateral boundary. While the first condition is trivially satisfied, the second condition requires

$$[\partial_1 u_1^0]_{x_1=\pm w} = \frac{\lambda \Delta}{\alpha t} \tag{41}$$

which leads to

$$a_{10} = \frac{\lambda}{\alpha}\frac{\Delta}{t}\frac{1}{\beta_{10}\cosh(\beta_{10} w)} \tag{42}$$

Then, the displacements $u_i (i = 1, 2)$ and the effective compression modulus E_c can be computed from the first of Eqs. (33) and (34) as, in view of Eqs. (37) and (38),

$$\begin{aligned} u_1 &= \frac{3}{2}\frac{\Delta}{t}\frac{\lambda}{\alpha}\frac{\sinh(\beta_{10} x_1)}{\beta_{10}\cosh(\beta_{10} w)}\left(1 - \frac{4x_2^2}{t^2}\right), \quad u_2 = -\frac{\Delta}{t} x_2 \\ E_c &= \alpha - \frac{\lambda^2}{\alpha}\frac{\tanh(\beta_{10} w)}{(\beta_{10} w)} \end{aligned} \tag{43}$$

It is noteworthy that the effect of compressibility is naturally included in the formulation. The above expressions clearly indicate that the zeroth order theory, which is the lowest order theory, simply corresponds to the averaging the field variables and equations over the layer thickness. Therefore, for compressive stiffness, it gives the same expression obtained by Tsai and Lee (1998). The selection of polynomial functions as distribution functions leads to a parabolic bulging shape in zeroth order theory. However, it may be noted that when the order of the theory is increased, the bulging shape will no longer be parabolic and, in fact, approaches the actual shape as dictated by the approximate theory.

4.1.1.2. Solution for first order theory. In the first order theory ($m = 1$, $p = 0$ and $p' = 1$), the governing equations should be analyzed both for $n = 0$ and $n = 1$, separately. It may be seen that, for $n = 0$, the governing equations for the first order theory are identical to those derived from the zeroth order theory. That is, the expression obtained for u_1^0 remains unchanged and Eqs. (40) and (42) are still valid. Considering Eq. (22) and Tables 1 and 2 for the first order theory and recalling from the zeroth order theory that

$$\tau_{22}^0 = \lambda \partial_1 u_1^0 - \frac{\alpha \Delta}{t} \tag{44}$$

the additional variable u_2^1 can be obtained from the solution of nontrivial equilibrium equation in x_2 direction for $n = 1$ (third of Eq. (21)), that is, from

$$\mu\left(\partial_{11} u_2^1 - \frac{60\alpha}{\mu t^2} u_2^1\right) - \frac{2}{t}(\lambda + \mu)(\partial_1 u_1^0) - \frac{10\alpha\Delta}{\mu t^2} = 0 \tag{45}$$

Necessary boundary condition for the solution of the above differential equation comes from the nontrivial boundary condition that $\tau_{12}^1|_{x_1=\pm w} = 0$, which yields

$$[\partial_1 u_2^1]_{x_1=\pm w} = \frac{2}{t}[u_1^0]_{x_1=\pm w} \tag{46}$$

Substituting Eqs. (40) and (42) into Eqs. (45) and (46), one gets the following governing equation and boundary condition for u_2^1:

$$\partial_{11} u_2^1 - \beta_{21}^2 u_2^1 = \frac{2}{t}\frac{\lambda + \mu}{\mu}\frac{\lambda}{\alpha}\frac{\Delta}{t}\frac{\cosh(\beta_{10} x_1)}{\cosh(\beta_{10} w)} + \frac{10\alpha\Delta}{\mu t^2} \tag{47}$$

with

$$[\partial_1 u_2^1]_{x_1=\pm w} = \pm\frac{2}{t}\frac{\lambda}{\alpha}\frac{\Delta}{t}\frac{\tanh(\beta_{10} w)}{\beta_{10}} \tag{48}$$

where

$$\beta_{10}^2 = \frac{12\mu}{\alpha t^2}, \quad \beta_{21}^2 = \frac{60\alpha}{\mu t^2} \tag{49}$$

The solution of Eq. (47) for u_2^1 subject to the boundary condition in Eq. (48) is

$$u_2^1 = a_{21}\cosh(\beta_{21}x_1) + \frac{2}{t}\frac{\mu+\lambda}{\mu}\frac{\lambda}{\alpha}\frac{\Delta}{t}\frac{1}{\beta_{10}^2-\beta_{21}^2}\frac{\cosh(\beta_{10}x_1)}{\cosh(\beta_{10}w)} - \frac{\Delta}{6} \tag{50}$$

where the integration constant a_{21} is given by

$$a_{21} = \frac{2}{t}\frac{\lambda}{\alpha}\frac{\Delta}{t}\frac{1}{\beta_{10}\beta_{21}}\frac{\tanh(\beta_{10}w)}{\sinh(\beta_{21}w)}\left[1 - \frac{\mu+\lambda}{\mu}\frac{\beta_{10}^2}{\beta_{10}^2-\beta_{21}^2}\right] \tag{51}$$

Then, the displacement distributions and effective compression modulus can be obtained through the use of the second of Eqs. (33) and Eq. (34) as, in view of the second of Eqs. (37) and first of Eqs. (38),

$$\begin{aligned} u_1 &= \frac{3}{2}\frac{\Delta}{t}\frac{\lambda}{\alpha}\frac{\sinh(\beta_{10}x_1)}{\beta_{10}\cosh(\beta_{10}w)}\left(1-\frac{4x_2^2}{t^2}\right) \\ u_2 &= \begin{bmatrix} \dfrac{30}{t}\dfrac{\lambda}{\alpha}\dfrac{\Delta}{t}\left\{\dfrac{1}{\beta_{10}\beta_{21}}\dfrac{\tanh(\beta_{10}w)}{\sinh(\beta_{21}w)}\left[1-\dfrac{\mu+\lambda}{\mu}\dfrac{\beta_{10}^2}{\beta_{10}^2-\beta_{21}^2}\right]\cosh(\beta_{21}x_1)\right. \\ \qquad \left. +\dfrac{\mu+\lambda}{\mu}\dfrac{1}{\beta_{10}^2-\beta_{21}^2}\dfrac{\cosh(\beta_{10}x_1)}{\cosh(\beta_{10}w)}\right\}\dfrac{x_2}{t}\left(1-\dfrac{4x_2^2}{t^2}\right) \\ -\frac{\Delta}{t}x_2 \end{bmatrix} \\ E_c &= \alpha - \frac{\lambda^2}{\alpha}\frac{\tanh(\beta_{10}w)}{(\beta_{10}w)} \end{aligned} \tag{52}$$

When the solutions in Eqs. (52) obtained by the first order theory are compared with those derived from the zeroth order theory (Eq. (43)), it may be seen that increasing the order of the theory from zero to one eliminates the common assumption used in literature, namely, plane horizontal section remains plane during deformation. On the other hand, parabolic bulging assumption is still included in the resulting expressions. At this stage, it is valuable to check the validity of these two commonly used assumptions by comparing the analytical predictions of the first order theory (FOT) with the results of the boundary element method (BEM).

Fig. 2a and b compare the predictions of analytical solutions (plotted in continuous lines) with BEM results (plotted as discrete points) for a shape factor of $S = 5.0$. Displacement distributions are plotted for four different values of Poisson's ratio; 0.3, 0.45, 0.49 and 0.499, so that the effect of compressibility on the layer behavior can also be studied. Since both over the bonded faces and at the central plane, plane sections remain plane, it is quite reasonable to investigate the axial displacement distribution along the width of the layer at the level of quarter thickness (i.e., at $x_2 = \pm t/4$). It is noticeable that while the assumption that plane sections remain plane seems to be somewhat reasonable for highly compressible ($\nu = 0.3$) materials, for materials with larger Poisson's ratio, this assumption is not valid as shown in Fig. 2a. The agreement between the analytical solutions and BEM results is very good for all studied values of Poisson's ratio. On the other hand, the parabolic bulging assumption can be accepted as a very realistic assumption as shown in Fig. 2b unless shape factor is too low.

It is to be noted that the use of zeroth and first order theories seems to be suitable for shape factors $S \geqslant 1.0$, where the bulging shape is known to be approximately parabolic. For very low shape factors ($S \ll 1.0$), where the bulging pattern is no longer parabolic, the order of the approximate theory should

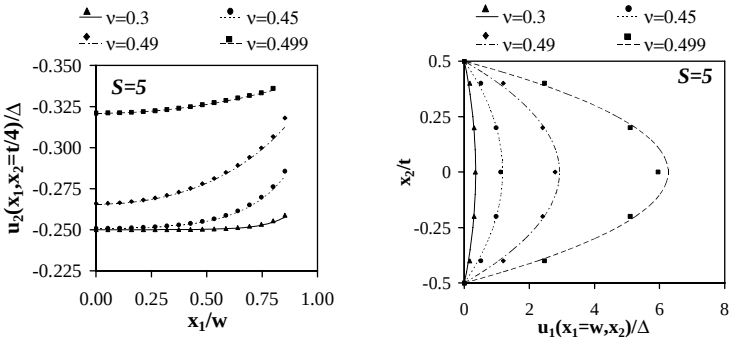

a. Assumption that plane sections remain plane

b. Parabolic bulging assumption

Fig. 2. Assessment of validity of two basic assumptions through the comparison of FOT (continuous lines) and BEM (discrete points) predictions for $S = 5$.

be increased. It is obvious that the increase of the order of the theory to two will release the kinematic assumption made in literature on bulging pattern. However, it may be noted that the governing equations of the second order theory (not presented in this study) are more complex and coupled, which seems to cause difficulties in the derivation of closed form solutions. This will be the subject of a later study.

4.1.2. Pure bending

For bending problem, in view of Eqs. (15) and (26), the first order theory has two nontrivial equations for two unknown weighted displacements, u_1^0 and u_2^1. The first equation comes from the first of Eqs. (26) with $n = 0$, which reduces to the following governing equation for u_1^0, in view of Eq. (22) and Tables 1 and 2 for $m = 1$,

$$\partial_{11}u_1^0 - \beta_{10}^2 u_1^0 = -\frac{\lambda+\mu}{\alpha}\frac{\phi}{t} \quad \text{where } \beta_{10}^2 = \frac{12\mu}{\alpha t^2} \tag{53}$$

Necessary boundary condition for the solution of Eq. (53) for u_1^0 is: $\tau_{11}^0|_{x_1=\pm w} = 0$, which requires

$$[\partial_1 u_1^0]_{x_1=\pm w} = -\frac{\lambda}{\alpha}\frac{\phi}{t}(\pm w) \tag{54}$$

Then, one has, for u_1^0,

$$u_1^0 = -\frac{\lambda}{\alpha}\frac{\phi}{t}\frac{w\cosh(\beta_{10}x_1)}{\beta_{10}\sinh(\beta_{10}w)} + \frac{\mu+\lambda}{12\mu}\phi t \tag{55}$$

The second equation for u_2^1 comes from the third of Eqs. (26) for $n = 1$. Considering Eq. (22) and Tables 1 and 2 for $m = 1$, the second of Eqs. (27) for $n = 0$, and Eq. (55) for u_1^0, the equation for u_2^1 reduces to

$$\partial_{11}u_2^1 - \beta_{21}^2 u_2^1 = -\frac{2}{t}\frac{\lambda+\mu}{\mu}\frac{\lambda}{\alpha}\frac{\phi}{t}\frac{w\sinh(\beta_{10}x_1)}{\sinh(\beta_{10}w)} - \frac{10\alpha}{\mu t^2}\phi x_1 \quad \text{with } \beta_{21}^2 = \frac{60\alpha}{\mu t^2} \tag{56}$$

Nontrivial boundary condition at the lateral sides: $\tau_{12}^1|_{x_1=\pm w} = 0$ yields

$$[\partial_1 u_2^1]_{x_1=\pm w} = -\frac{2}{t}\frac{\lambda}{\alpha}\frac{\phi}{t}\frac{w}{\beta_{10}\tanh(\beta_{10}w)} + \frac{\mu+\lambda}{6\mu}\phi \tag{57}$$

Using this boundary condition, u_2^1 may be determined as

$$u_2^1 = a_{22}\sinh(\beta_{21}x_1) - \frac{2}{t}\frac{\mu+\lambda}{\mu}\frac{\lambda}{\alpha}\frac{\phi}{t}\frac{1}{\beta_{10}^2-\beta_{21}^2}\frac{w\sinh(\beta_{10}x_1)}{\sinh(\beta_{10}w)} + \frac{\phi}{6}x_1 \tag{58}$$

where the integration constant a_{22} is given by

$$a_{22} = -\frac{2}{t}\frac{\lambda}{\alpha}\frac{\phi}{t}\frac{w}{\beta_{10}\beta_{21}}\frac{\coth(\beta_{10}w)}{\cosh(\beta_{21}w)}\left[1-\frac{\mu+\lambda}{\mu}\frac{\beta_{10}^2}{\beta_{10}^2-\beta_{21}^2}\right]+\frac{\phi}{6}\frac{\lambda}{\mu}\frac{1}{\beta_{21}\cosh(\beta_{21}w)} \tag{59}$$

Then, the displacement components u_i and effective bending modulus E_b may be obtained from the second of Eqs. (33) and Eq. (35) as, in view of the second of Eqs. (37) and first of Eqs. (38),

$$u_1 = \left[-\frac{3}{2}\frac{\lambda}{\alpha}\frac{\phi}{t}\frac{w\cosh(\beta_{10}x_1)}{\beta_{10}\sinh(\beta_{10}w)}+\frac{\mu+\lambda}{8\mu}\phi t\right]\left(1-\frac{4x_2^2}{t^2}\right)$$

$$u_2 = \left\{\begin{array}{l}\left(\begin{array}{l}-\dfrac{30}{t}\dfrac{\lambda}{\alpha}\dfrac{\phi}{t}\dfrac{w}{\beta_{10}\beta_{21}}\dfrac{\coth(\beta_{10}w)}{\cosh(\beta_{21}w)}\left[1-\dfrac{\mu+\lambda}{\mu}\dfrac{\beta_{10}^2}{\beta_{10}^2-\beta_{21}^2}\right]\sinh(\beta_{21}x_1)\\ +\dfrac{5\phi}{2}\dfrac{\lambda}{\mu}\dfrac{\sinh(\beta_{21}x_1)}{\beta_{21}\cosh(\beta_{21}w)}-\dfrac{30}{t}\dfrac{\lambda}{\alpha}\dfrac{\phi}{t}\dfrac{\mu+\lambda}{\mu}\dfrac{w}{\beta_{10}^2-\beta_{21}^2}\dfrac{\sinh(\beta_{10}x_1)}{\sinh(\beta_{10}w)}\end{array}\right)\dfrac{x_2}{t}\left(1-\dfrac{4x_2^2}{t^2}\right)\\ -\dfrac{\phi}{t}x_1x_2\end{array}\right\} \tag{60}$$

$$E_b = \alpha-\frac{15\lambda\alpha}{\mu}\left\{\begin{array}{l}\dfrac{\mu+\lambda}{\mu}\dfrac{\beta_{10}^2}{\beta_{10}^2-\beta_{21}^2}\left[\begin{array}{l}\dfrac{1}{(\beta_{10}w)^2}\left(1-\dfrac{\beta_{10}w}{\tanh(\beta_{10}w)}\right)+\\ \dfrac{1}{(\beta_{21}w)^2}\dfrac{\beta_{10}w}{\tanh(\beta_{10}w)}\left(1-\dfrac{\tanh(\beta_{21}w)}{\beta_{21}w}\right)\end{array}\right]+\\ \dfrac{1}{(\beta_{21}w)^2}\left(1-\dfrac{\beta_{10}w}{\tanh(\beta_{10}w)}\right)\left(1-\dfrac{\tanh(\beta_{21}w)}{\beta_{21}w}\right)\end{array}\right\}$$

4.1.3. Apparent shear

When the first order theory is applied to the apparent shear problem, one has, in view of Eq. (30), two unknown weighted displacements; u_2^0 and u_1^1. The governing equation for u_2^0 comes from the third of Eqs. (31) for $n=0$, which, in view of Eq. (22) and Tables 1 and 2 for $m=1$, simplifies to

$$\partial_{11}u_2^0-\beta_{20}^2u_2^0=0 \quad \text{where } \beta_{20}^2=\frac{12\alpha}{\mu t^2} \tag{61}$$

From the nontrivial boundary condition $\tau_{12}^0|_{x_1=\pm w}=0$, one also has

$$[\partial_1 u_2^0]_{x_1=\pm w}=-\frac{\delta}{t} \tag{62}$$

Thus, u_2^0 becomes

$$u_2^0=-\frac{\delta}{t}\frac{\sinh(\beta_{20}x_1)}{\beta_{20}\cosh(\beta_{20}w)} \tag{63}$$

For $n=1$, the only nontrivial equation is the first of Eqs. (31). Considering Eq. (22) and the coefficients given in Tables 1 and 2 for $m=1$, the second of Eqs. (32) for n = 0, and Eq. (63) for u_2^0, the governing equation for u_1^1 is obtained as

$$\partial_{11}u_1^1-\beta_{11}^2u_1^1=-\frac{2}{t}\frac{\lambda+\mu}{\alpha}\frac{\delta}{t}\frac{\cosh(\beta_{20}x_1)}{\cosh(\beta_{20}w)}-\frac{10\mu}{\alpha t^2}\delta \quad \text{with} \quad \beta_{11}^2=\frac{60\mu}{\alpha t^2} \tag{64}$$

Nontrivial boundary condition at the lateral sides: $\tau_{11}^1|_{x_1=\pm w} = 0$ requires

$$[\partial_1 u_1^1]_{x_1=\pm w} = -\frac{2}{t}\frac{\lambda}{\alpha}\frac{\delta}{t}\frac{\tanh(\beta_{20}w)}{\beta_{20}} \tag{65}$$

Then, one obtains u_1^1 as

$$u_1^1 = a_{11}\cosh(\beta_{11}x_1) - \frac{2}{t}\frac{\mu+\lambda}{\alpha}\frac{\delta}{t}\frac{1}{\beta_{20}^2-\beta_{11}^2}\frac{\cosh(\beta_{20}x_1)}{\cosh(\beta_{20}w)} + \frac{\delta}{6} \tag{66}$$

where

$$a_{11} = -\frac{2}{t}\frac{\lambda}{\alpha}\frac{\delta}{t}\frac{1}{\beta_{11}\beta_{20}}\frac{\tanh(\beta_{20}w)}{\sinh(\beta_{11}w)}\left[1-\frac{\mu+\lambda}{\lambda}\frac{\beta_{20}^2}{\beta_{20}^2-\beta_{11}^2}\right] \tag{67}$$

Consequently, the displacement components u_i and apparent shear modulus μ_a are evaluated from the second of Eqs. (33) and (36) as, in view of Eqs. (37) and (38),

$$\begin{aligned}
u_1 &= \left(-\frac{30}{t}\frac{\lambda}{\alpha}\frac{\delta}{t}\frac{\tanh(\beta_{20}w)}{\beta_{11}\beta_{20}}\frac{\cosh(\beta_{11}x_1)}{\sinh(\beta_{11}w)}\left[1-\frac{\mu+\lambda}{\lambda}\frac{\beta_{20}^2}{\beta_{20}^2-\beta_{11}^2}\right] - \frac{30}{t}\frac{\mu+\lambda}{\alpha}\frac{\delta}{t}\frac{1}{\beta_{20}^2-\beta_{11}^2}\frac{\cosh(\beta_{20}x_1)}{\cosh(\beta_{20}w)}\right)\frac{x_2}{t}\left(1-\frac{4x_2^2}{t^2}\right)+\frac{\delta}{t}x_2 \\
u_2 &= \left[-\frac{3}{2}\frac{\delta}{t}\frac{\sinh(\beta_{20}x_1)}{\beta_{20}\cosh(\beta_{20}w)}\right]\left(1-\frac{4x_2^2}{t^2}\right) \\
\mu_a &= \mu\left[1-\frac{\tanh(\beta_{20}w)}{(\beta_{20}w)}\right]
\end{aligned} \tag{68}$$

4.2. Discussions of analytical solutions

Knowing the expressions for displacement distributions, expressions for stress distributions can be obtained from stress–displacement relations of linear elasticity. Analytical solutions derived using the approximate theory can be used to plot the displacement/stress distributions at any section of an infinite-strip-shaped elastic bonded layer under its three basic deformation modes or under any combinations of these modes. In addition, the effects of two main parameters, shape factor (S) and Poisson's ratio (ν), on the layer behavior, that is, on the displacement/stress distributions or magnitudes/locations of maximum stresses developed in the layer or on its compression/bending/apparent shear modulus, can be studied thoroughly.

4.2.1. Compressive behavior

Fig. 3 illustrates the effect Poisson's ratio on lateral normal and shear stress distributions through the layer thickness under uniform compression. To be able to see the effect of shape factor besides Poisson's ratio, stress distributions are plotted for two different shape factors; $S = 1$, representing low shape factor (LSF) layers, and $S = 30$ representing considerably high shape factor (HSF) layers. It is to be noted that the shape factor of a layer of infinite-strip shape with a thickness of t and width of $2w$ equals to the ratio of its half-width to its thickness; i.e., $S = w/t$. To study the behavior of a bonded layer over a wide range of compressibility, stress distributions are plotted for $\nu \cong 0.5$, 0.499, 0.45 and 0.3.

In Fig. 3, lateral normal stress distributions are plotted along the centerline ($x_1 = 0$), where it takes its maximum value. It is known that, under uniform compression, shear stress increases in horizontal direction

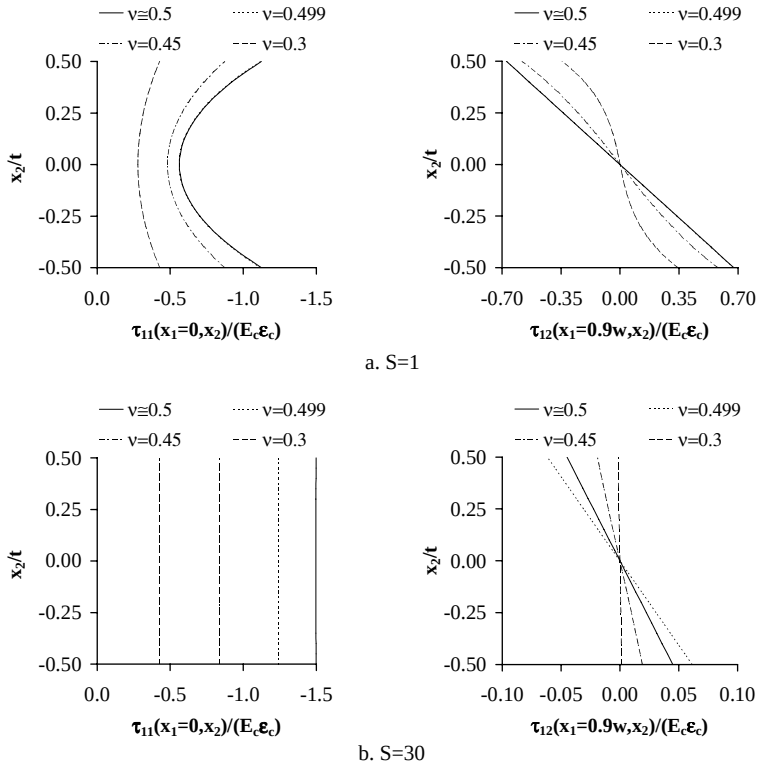

Fig. 3. Effect of Poisson's ratio on lateral normal and shear stress distributions through the layer thickness under uniform compression.

as moved from centroid to the edges, where it suddenly drops to zero due to the stress-free boundary conditions. It is also known that stress singularities observed at the edges are usually confined to a very limited region (Gent et al., 1974). Therefore, shear stress distributions given in Fig. 3 are plotted along the vertical axis at $x_1 = 0.9w$, which is thought to be sufficiently away from the load-free edge and at the same time adequately close to the points where shear stresses are maximum. It should also be noted that, in the plots, stress values are normalized with respect to the uniform pressure, i.e. $E_c\varepsilon_c$.

As shown in the plots, while lateral normal stress is constant through the layer thickness for $S = 30$, it has a parabolic variation for $S = 1$. It is to be observed that this is the prediction of the first order theory and is valid, as noted before, when $S \geqslant 1$. The behavior of the LSF layer is also different from that of HSF layer in that while considerable shear stress develops in the region close to the outer boundary for $S = 1$, it is almost negligible for $S = 30$. Shear stress distribution is linear, even for $S = 1$, for nearly incompressible materials. On the other hand, as material becomes compressible, the distribution looses its linearity for the LSF layer. It is also remarkable that, for $S = 1$, incompressible behavior is attained at $v = 0.499$ whereas stress values are much more sensitive to the changes in material properties for $S = 30$.

Fig. 4 contains some results for maximum axial and shear stresses. Our study indicated that stress components reach their maximum values at different but fixed locations. While $(\tau_{22})_{\max}$ occurs at $(x_1 = 0, x_2 = 0)$, $(\tau_{11})_{\max}$ occurs at $(x_1 = 0, x_2 = \pm t/2)$ and $(\tau_{12})_{\max}$ at $(x_1 = \pm w, x_2 = \pm t/2)$. It is also observed that the magnitudes of maximum stresses are functions of both shape factor and Poisson's ratio. As shown in Fig. 4a, $(\tau_{22})_{\max}$ for an incompressible layer increases with shape factor until it reaches to a peak value of 1.5 $E_c\varepsilon_c$ at about $S = 10$, beyond which it remains constant. The behavior of compressible layers is

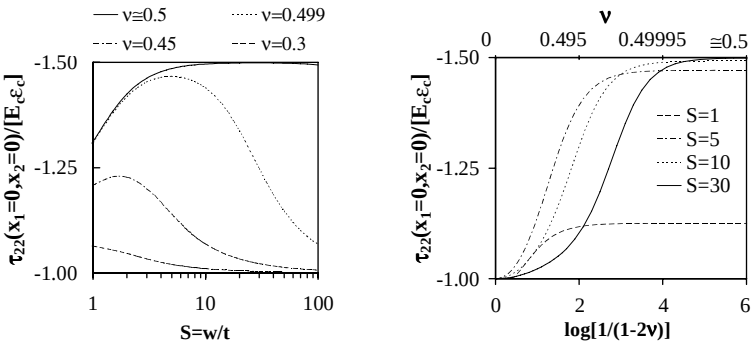

a. Maximum axial stress

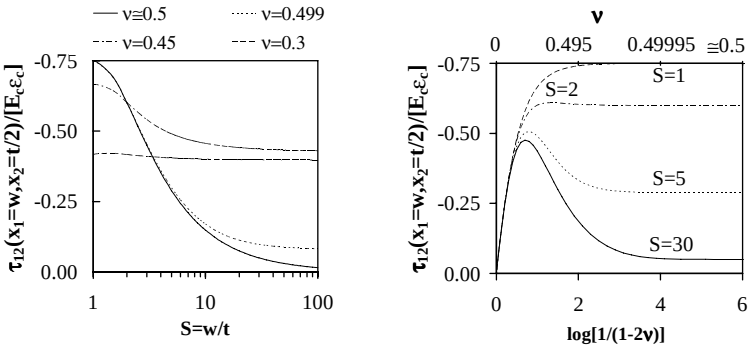

b. Maximum shear stress

Fig. 4. Effect of shape factor and Poisson's ratio on maximum axial and shear stresses under uniform compression.

considerably different from this incompressible behavior: for compressible layer, $(\tau_{22})_{max}$ reaches its peak value at a critical shape factor smaller than $S = 10$ depending on the compressibility of the material; beyond the critical value of shape factor, $(\tau_{22})_{max}$ softens with increasing S. The significance in the decrease is affected from Poisson's ratio. The effect of Poisson's ratio on the value of $(\tau_{22})_{max}$ is more apparent in the second of Fig. 4a. In the studied range of shape factors, $(\tau_{22})_{max}$ increases with increasing Poisson's ratio until the limiting incompressible value is approached. The lower the shape factor, the lower the value of Poisson's ratio at which the plateau is reached. This is consistent with the earlier observation that stresses developed in LSF layers are not influenced much by the changes in Poisson's ratio close to 0.5.

Similar to the axial stress, $(\tau_{12})_{max}$ attains its maximum value at very low shape factors, typically at $S = 1$ for $\nu \geqslant 0.45$ (Fig. 4b). For this critical shape factor, the magnitude of $(\tau_{12})_{max}$ is observed to increase as incompressibility is approached. For $\nu \geqslant 0.45$, as shape factor increases beyond $S = 1$, the magnitude of $(\tau_{12})_{max}$ decreases. The amount of decrease is much higher at nearly incompressible materials. When the effect of Poisson's ratio on $(\tau_{12})_{max}$ is studied carefully, it is recognized that for about $\nu \geqslant 0.4$, $(\tau_{12})_{max}$ developed in an elastic bonded layer of $S = 1$ is always the highest in the range of $S \geqslant 1$. For $S > 1$, after the maximum is reached, $(\tau_{12})_{max}$ starts to decrease with increasing Poisson's ratio until the incompressible behavior is reached.

4.2.2. Bending behavior

Although the derivation is not included in Section 4.1.2, it is not difficult to show that the zeroth order theory leads to the same expression for bending modulus derived by Tsai and Lee (1999) for infinite-

strip-shaped bonded elastic layers. Fig. 5 compares the predictions of zeroth and first order theories for bending modulus. As shown in the figure, the predictions of zeroth and first order theories exactly match in the studied range of parameters.

In design calculations, it is a common practice to represent the effective bending modulus E_b of a bonded elastic layer in terms of its compression modulus E_c. A factor of five (Chalhoub and Kelly, 1991) is used for the ratio of E_c to E_b for infinite-strip-shaped bonded layers. In Fig. 6, the E_c/E_b ratio is plotted for infinite-strip-shaped bonded layers with different shape factors and Poisson's ratios using the third of Eq. (52) and third of Eq. (60). As shown in the figure, the above-mentioned value of five is only valid for incompressible materials and for considerably high shape factors. For instance, for $\nu = 0.499$ and for $S > 5$, as shape factor increases, this value of ratio will significantly underestimate the true value of bending modulus.

Similar to the compression problem, for pure bending problem, stress distributions or maximum stresses can be plotted for different values of shape factor and Poisson's ratio to investigate the effects of these two important parameters on the layer behavior. In this section, only maximum hydrostatic tension developing in an infinite-strip-shaped layer under pure bending is investigated for the study of "internal rupture"

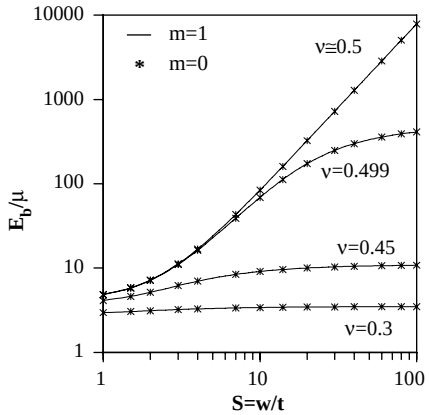

Fig. 5. Predictions of zeroth and first order theories for bending modulus.

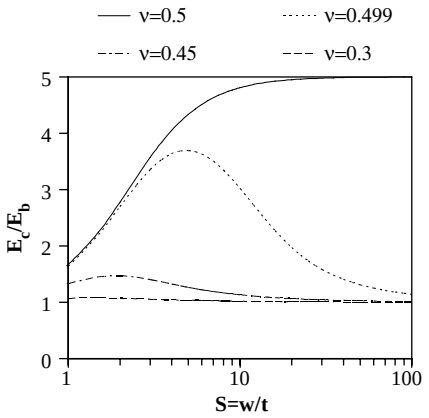

Fig. 6. Effect of Poisson's ratio and shape factor on E_c/E_b ratio.

phenomena, which is one of the failure modes a bonded rubber layer can undergo under pure bending (Gent and Meinecke, 1970; Horton et al., 2002b). Internal rupture of a rubber layer is defined by Gent and Meinecke (1970) as the failure of the layer in such a way that "any small cavity will increase indefinitely in size" when the magnitude of hydrostatic tension exceeds a critical value, typically $3/4E$ where E is the Young's modulus of the rubber. Using the pressure approach of Gent and Lindley (1959), Gent and Meinecke (1970) obtained the following values for the location (x_1^*) and magnitude (ϕ^*) of critical rotation at which an infinite-strip-shaped bonded rubber layer will fail due to internal rupture under pure bending:

$$x_1^* = \frac{w}{\sqrt{3}} \quad \text{and} \quad \phi^* = \frac{27\sqrt{3}}{16S^3} \tag{69}$$

It should be recognized that these values are derived based on the incompressibility assumption. However, as it can be shown, Poisson's ratio has significant effect on stress values. At this point, it should be emphasized that, unlike the compression case, in a bonded elastic layer subjected to pure bending, normal stresses may reach their maximum values at different locations at a specific horizontal section and that their exact locations highly depend on shape factor and Poisson's ratio. In other words, the maximum normal stress components developed in a bonded elastic layer subject to pure bending have not fixed, but varied locations depending on the geometric and material properties of the layer. Our study based on first order theory indicated that the maximum pressure occurs at locations where the lateral normal stress reaches its maximum value.

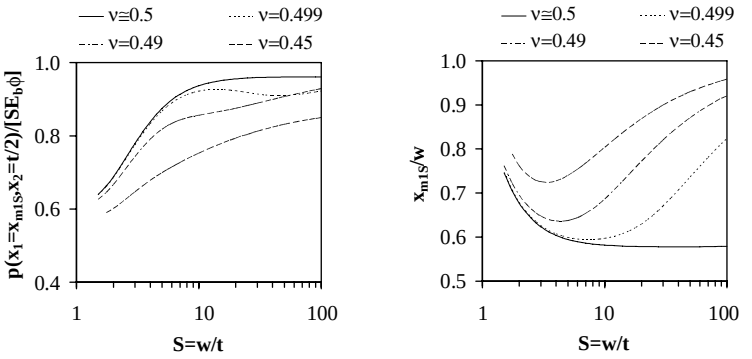

a. variation with respect to shape factor

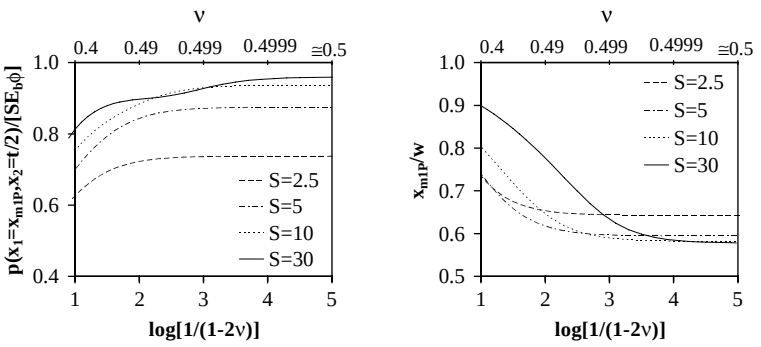

b. variation with respect to Poisson's ratio

Fig. 7. Effect of shape factor and Poisson's ratio on the location and magnitude of maximum pressure under pure bending.

Fig. 7 shows the effects of shape factor and Poisson's ratio on both the location, denoted as x_{m1S} or x_{m1P}, and magnitude of maximum pressure. Pressure values are normalized by $SE_b\phi$ which corresponds to the maximum bending stress developed in the corresponding unbonded layer predicted by simple beam theory as noted by Tsai (2003). As shown in the figure, shape factor and Poisson's ratio have significant influence on both the location and magnitude of maximum pressure. $x_{m1S} = x_1^*$ holds only for considerably high shape factors and incompressible materials. For lower shape factors, the site of failure moves towards the edge of the layer as shape factor decreases.

4.2.3. Apparent shear behavior

As mentioned before, although some researchers (e.g., Rivlin and Saunders, 1949; Horton et al., 2002b) obtained approximate expressions for apparent shear modulus of bonded elastic layers, these expressions were all derived based on the assumption that plane sections remain plane. Moreover, they only considered incompressible materials. Using the first order theory presented in this study eliminates both of these assumptions but has retained the parabolic lateral surfaces assumptions. The resulting expression is functions of both shape factor and Poisson's ratio. It seems to be beneficial to study the effects of each parameter on the apparent shear modulus.

In Fig. 8 the variation of the ratio of apparent shear modulus to true shear modulus (μ_a/μ) with each parameter is given. From the figure it is clear that, for incompressible materials, the apparent shear modulus of a bonded elastic layer equals its true shear modulus and is independent of the value of shape factor. Fig. 8 also shows that the effect of compressibility becomes important only if shape factor is considerably small. This result is compatible with the common acceptance that while the compressive and bending behavior of a bonded rubber layer can be considerably different than the behavior of corresponding unbonded layer, the effect of the bonded surfaces to its shear behavior is negligible. Layers of high shape factors are almost insensitive to the changes in Poisson's ratio. On the other hand, for low shape factors like $S = 0.5$, apparent shear modulus decreases considerably with decreasing Poisson's ratio.

As far as displacement and stress distributions are concerned, it is valuable to compare the analytical predictions of first order theory (FOT) with the numerical results of boundary element method (BEM). Figs. 9 and 10 illustrate displacement and stress distributions in a bonded elastic strip with a shape factor of $S = 1$ and for $\nu = 0.3$. It is remarkable that analytical predictions of FOT for both displacement and stress distributions are in very good agreement with the BEM results. It is also worth noting that $\mu_{a,\,\mathrm{BEM}} = 0.848$ while $\mu_{a,\,\mathrm{FOT}} = 0.846$ for the considered S and ν values.

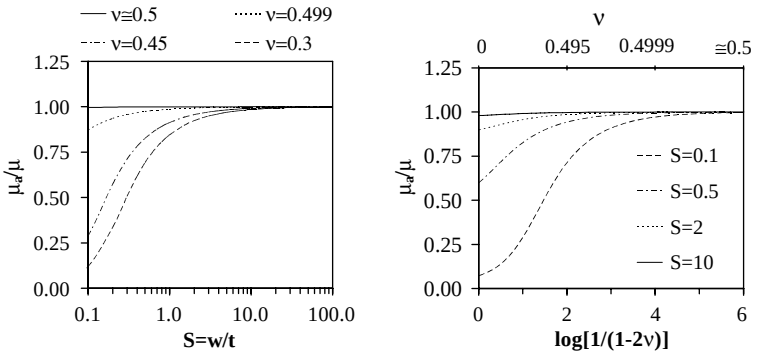

Fig. 8. Effect of shape factor and Poisson's ratio on apparent shear modulus.

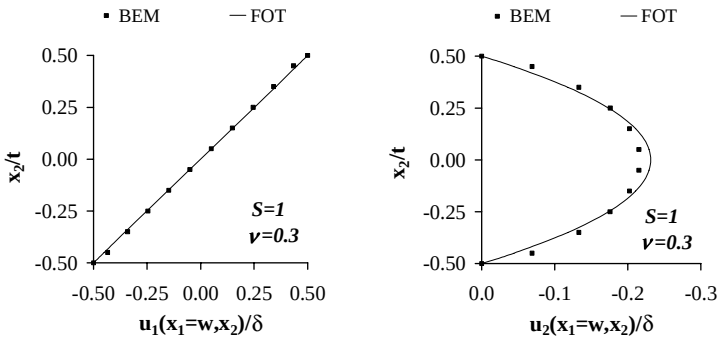

Fig. 9. Displacement distributions under apparent shear.

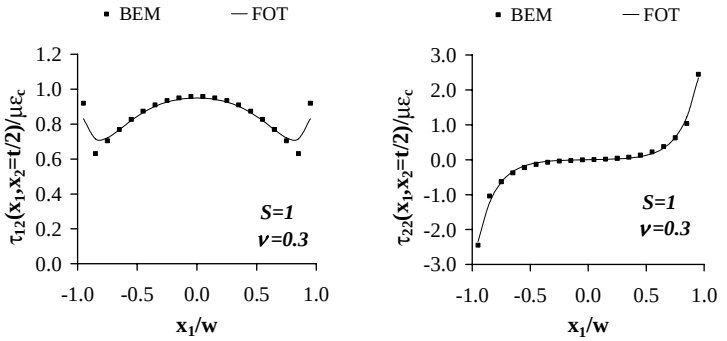

Fig. 10. Stress distributions at the bonded faces under apparent shear.

5. Conclusions

In this study, behavior of bonded elastic layers under three fundamental deformation states, uniform compression, pure bending and apparent shear, is formulated by using the approximate theory based on modified Galerkin method developed by Mengi (1980). Selecting Legendre polynomials as distribution functions and retaining the order of the theory arbitrary, most general forms of governing equations are obtained for the analysis. The formulation can easily be applied to a bonded elastic layer by specifying the geometric and material properties of the layer and selecting the order of the theory. After the solution of governing equations for unknown weighted displacements, determination of displacement/stress distributions or any other parameter, such as, stiffness of the layer is straightforward as explained in Sections 3.2 and 3.3. The application of the formulation is exemplified by solving the governing equations for infinite-strip-shaped layers. For each deformation mode, closed form expressions are derived for displacement/stress distributions and relevant effective modulus.

It has been realized that due to the use of polynomial functions, the zeroth order theory leads to the same expressions that have been derived in literature based on two kinematics assumptions: the plane sections remain plane and parabolic bulging (e.g., see Tsai and Lee, 1998, 1999). The increase of the order of the theory to one is shown to eliminate the first kinematics assumption, retaining solely the parabolic bulging assumption. Governing equations clearly reveal that the second order theory also removes this last

assumption. It is not always possible to derive closed form solutions in the case of higher order theories due to the complex and coupled forms of governing equations.

Analytical solutions derived using the approximate theory can be used to determine the displacement/stress distributions at any section of an infinite-strip-shaped elastic bonded layer under its three basic deformation modes and also under their combinations, and to study the effects of two main parameters, shape factor and Poisson's ratio, on the layer behavior. The following conclusions may be drawn for the behavior of infinite-strip-shaped elastic layers bonded to rigid surfaces from the solutions obtained through first order theory.

- Shape factor and Poisson's ratio are the two basic parameters controlling the behavior of a bonded elastic layer. They have significant effects not only on its stiffnesses but also on the displacement/stress distributions and on the magnitudes and/or locations of the maximum stresses.
- Stress assumptions of the pressure method in uniform compression case appear to be valid only for HSF layers. These assumptions involve assuming uniform distribution for normal stresses and linear distribution for shear stress over the thickness of the layer, which are inconsistent with the results presented in Fig. 3 for LSF layers.
- LSF layers under uniform compression reach their incompressible behavior at a Poisson's ratio of about $v = 0.499$. On the other hand, stress values are much more sensitive to the value of Poisson's ratio for HSF layers, even for nearly incompressible materials. For example, the use of $1.5E_c\varepsilon_c$ for the maximum value of normal stress (by assuming incompressible behavior) will be very misleading for HSF layers. It is also worth noting that for about $v \geqslant 0.4$, the maximum shear stress developing in a layer of $S = 1$ is always the highest in the range of $S \geqslant 1$.
- It is shown that the predictions of zeroth and first order theories for bending modulus match exactly for $S \geqslant 1$. Considering the complexity of the expression predicted by first order theory, the simpler formula of zeroth order theory is suggested for the use in design calculations. Also, a care should be taken if one prefers to express the bending stiffness of a bonded elastic layer in terms of its compression modulus in design calculations. Using the incompressible value of 5 for E_c/E_b ratio will seriously underestimate the true value of bending modulus, even if a compressible formulation is used in the calculation of E_c, especially for compressible HSF layers.
- Determination of the magnitudes and locations of maximum hydrostatic tension developing in a bonded elastic layer subject to bending is essential for investigating its internal rupture behavior. It is shown that the prediction of Gent and Meinecke (1970) is valid only for incompressible HSF layers. For lower shape factors or compressible materials, the site of failure shifts towards the edge of the layer and the value of maximum hydrostatic tension gets smaller.
- The theory is also capable of formulating the apparent shear problem. The closed form solutions obtained using the first order theory may be thought to be the first trial solution for apparent shear behavior of bonded elastic layers of compressible materials. When plotted with respect to Poisson's ratio and shape factor, it is found that the apparent shear modulus not only depends on the geometric properties of the layer but is also affected significantly from the compressibility of the material especially if the shape factor of the layer is considerably low.

Acknowledgement

This study is supported by METU Research Fund under grants AFP-2001-03-03-07 and BAP-2002-03-03-04.

References

Chalhoub, M.S., Kelly, J.M., 1990. Effect of bulk compressibility on the stiffness of cylindrical base isolation bearings. International Journal of Solids and Structures 26, 743–760.

Chalhoub, M.S., Kelly, J.M., 1991. Analysis of infinite-strip-shaped base isolator with elastomer bulk compression. Journal of Engineering Mechanics ASCE 117, 1791–1805.

Constantinou, M.S., Kartoum, A., Kelly, J.M., 1992. Analysis of compression of hollow circular elastomeric bearings. Engineering Structures 14, 103–111.

Fenner, R.T., Remzi, E.M., 1983. Boundary integral equation evaluation of compression moduli of bonded rubber blocks. Journal of Strain Analysis 18, 217–223.

Gent, A.N., Lindley, P.B., 1959. The compression of bonded rubber blocks. Proceedings of the Institution of Mechanical Engineers 173, 111–122.

Gent, A.N., Meinecke, E.A., 1970. Compression, bending and shear of bonded rubber blocks. Polymer Engineering and Science 10, 48–53.

Gent, A.N., Henry, R.L., Roxbury, M.L., 1974. Interfacial stresses for bonded rubber blocks in compression and shear. Journal of Applied Mechanics 41, 855–859.

Holownia, B.P., 1972. Effect of Poisson's ratio on bonded rubber blocks. Journal of Strain Analysis 7, 236–242.

Horton, J.M., Tupholme, G.E., Gover, M.J.C., 2002a. Axial loading of bonded rubber blocks. Journal of Applied Mechanics, ASME 69, 836–843.

Horton, J.M., Tupholme, G.E., Gover, M.J.C., 2002b. Bending of circular-section bonded rubber blocks. International Journal of Solids and Structures 39, 5879–5893.

Horton, J.M., Tupholme, G.E., Gover, M.J.C., 2003. Axial loading of annular bonded rubber blocks. Rubber Chemistry and Technology 76, 1194–1211.

Imbimbo, M., De Luca, A., 1998. F.E. stress analysis of rubber bearings under axial loads. Computers and Structures 68, 31–39.

Kelly, J.M., 1997. Earthquake Resistant Design with Rubber. Springer-Verlag, London.

Koh, C.G., Kelly, J.M., 1989. Compression stiffness of bonded square layers of nearly incompressible material. Engineering Structures 11, 9–15.

Koh, C.G., Lim, H.L., 2001. Analytical solution for compression stiffness of bonded rectangular layers. International Journal of Solids and Structures 38, 445–455.

Lindley, P.B., 1979a. Compression module for blocks of soft elastic material bonded to rigid end plates. Journal of Strain Analysis 14, 11–16.

Lindley, P.B., 1979b. Plane strain rotation module for of soft elastic blocks. Journal of Strain Analysis 14, 17–21.

Mengi, Y., 1980. A new approach for developing dynamic theories for structural elements Part 1: Application to thermoelastic plates. International Journal of Solids and Structures 16, 1155–1168.

Mott, P.H., Roland, C.M., 1995. Uniaxial deformation of rubber cylinders. Rubber Chemistry and Technology 68, 739–745.

Naeim, F., Kelly, J.M., 1999. Design of Seismic Isolated Structures. John Wiley & Sons.

Papoulia, K.D., Kelly, J.M., 1996. Compression of bonded soft elastic material: variational solution. Journal of Engineering Mechanics ASCE 122, 1791–1805.

Rivlin, R.S., Saunders, D.W., 1949. Cylindrical shear mountings. IRI Transactions 24, 249–306.

Tsai, H.-C., 2003. Flexure analysis of circular elastic layers bonded between rigid plates. International Journal of Solids and Structures 40, 2975–2987.

Tsai, H.-C., 2005. Compression analysis of rectangular elastic layers bonded between rigid plates. International Journal of Solids and Structures 42, 3395–3410.

Tsai, H.-C., Lee, C.C., 1998. Compressive stiffness of elastic layers bonded between rigid plates. International Journal of Solids and Structures 35, 3053–3069.

Tsai, H.-C., Lee, C.C., 1999. Tilting stiffness of elastic layers bonded between rigid plates. International Journal of Solids and Structures 36, 2485–2505.

Yeoh, O.H., Pinter, G.A., Banks, H.T., 2002. Compression of bonded rubber blocks. Rubber Chemistry and Technology 75, 549–561.